© 2016. Published by The Company of Biologists Ltd | Journal of Cell Science (2016) 129, 1329-1339 doi:10.1242/jcs.178855

RESEARCH ARTICLE

# Greatwall dephosphorylation and inactivation upon mitotic exit is triggered by PP1

**Sheng Ma[1,*], Suzanne Vigneron[1,*], Perle Robert[1], Jean Marc Strub[2], Sara Cianferani[2], Anna Castro[1,‡] and Thierry Lorca[1,‡]**

## ABSTRACT

Entry into mitosis is induced by the activation of cyclin-B–Cdk1 and Greatwall (Gwl; also known as MASTL in mammals) kinases. Cyclin-B–Cdk1 phosphorylates mitotic substrates, whereas Gwl activation promotes the phosphorylation of the small proteins Arpp19 and ENSA. Phosphorylated Arpp19 and/or ENSA bind to and inhibit PP2A comprising the B55 subunit (PP2A-B55; B55 is also known as PPP2R2A), the phosphatase responsible for cyclin-B–Cdk1 substrate dephosphorylation, allowing the stable phosphorylation of mitotic proteins. Upon mitotic exit, cyclin-B–Cdk1 and Gwl kinases are inactivated, and mitotic substrates are dephosphorylated. Here, we have identified protein phosphatase-1 (PP1) as the phosphatase involved in the dephosphorylation of the activating site (Ser875) of Gwl. Depletion of PP1 from meiotic *Xenopus* egg extracts maintains phosphorylation of Ser875, as well as the full activity of this kinase, resulting in a block of meiotic and mitotic exit. By contrast, preventing the reactivation of PP2A-B55 through the addition of a hyperactive Gwl mutant (GwlK72M) mainly affected Gwl dephosphorylation on Thr194, resulting in partial inactivation of Gwl and in the incomplete exit from mitosis or meiosis. We also show that when PP2A-B55 is fully reactivated by depleting Arpp19, this protein phosphatase is able to dephosphorylate both activating sites, even in the absence of PP1.

**KEY WORDS: Greatwall, PP1, PP2A-B55, Mitotic exit, Meiotic exit**

## INTRODUCTION

Entry into mitosis or meiosis requires the phosphorylation of a high number of mitotic proteins. This phosphorylation is mostly performed by the complex cyclin-B–Cdk1. However, mitotic substrate phosphorylation is also dependent on the activity of the phosphatase PP2A comprising the B55 subunit (PP2A-B55; B55 is also known as PPP2R2A PP2A-B55), which mediates dephosphorylation of such substrates. It is well established that the Greatwall kinase (Gwl; also known as MASTL in mammals) is activated at the G2/M transition by a first phosphorylation on the T-loop site (Thr193 in the *Xenopus* protein sequence; Thr194 in the human protein sequence) by cyclin-B–Cdk1, followed by an autophosphorylation of the C-terminal activating site (Ser883 in the *Xenopus* protein sequence; Ser875 in the human protein sequence) (Blake-Hodek et al., 2012; Vigneron et al., 2011). The activation of this kinase promotes the inhibition of PP2A-B55 through the phosphorylation of its substrates Arpp19 and ENSA (Alvarez-Fernandez et al., 2013; Gharbi-Ayachi et al., 2010; Lorca et al., 2010; Mochida et al., 2010). This inhibition results in the stable phosphorylation of cyclin-B–Cdk1 substrates and mitotic entry.

To return to the interphase state, proteins must be dephosphorylated. This dephosphorylation is dependent on the inactivation of cyclin-B–Cdk1 and the reactivation of the phosphatase PP2A-B55 (Mochida et al., 2009). Cyclin-B–Cdk1 inactivation is achieved by the anaphase-promoting complex/cyclosome (APC/C)-dependent degradation of cyclin B (Peters, 2006). PP2A-B55 reactivation depends on the inactivation of Gwl and the dephosphorylation of Arpp19 and ENSA. Recent data suggest that Gwl dephosphorylation and inactivation is mediated by the phosphatase PP2A-B55 (Hégarat et al., 2014). The identity of the phosphatase involved in Arpp19 and ENSA dephosphorylation is much less clear. Two different phosphatases have been suggested to be responsible, PP2A-B55 (Williams et al., 2014) and Fcp1 (also known as CTDP1) (Hégarat et al., 2014). Finally, both PP1 (Wu et al., 2009) and PP2A-B55 (Cundell et al., 2013; Mochida et al., 2009) have been shown to contribute to cyclin-B–Cdk1 substrate dephosphorylation. In this work, we investigate the role of different phosphatases in Gwl inactivation and cyclin-B–Cdk1 substrate dephosphorylation upon meiotic and mitotic exit.

## RESULTS

### PP2A-B55 and PP1 but not Fcp1 are required for a correct meiotic and mitotic exit

Fcp1 has been recently suggested to be responsible for Arpp19 and ENSA dephosphorylation, and to mediate in this way the exit of human cells from mitosis (Hégarat et al., 2014). We used *Xenopus* egg extracts that had been arrested in metaphase of meiosis II [cytostatic factor (CSF) extracts], as well as interphase egg extracts, to investigate the role of this phosphatase in inducing meiotic exit. With that aim, we performed Fcp1 or control depletions in CSF extracts and subsequently forced the extracts to exit meiosis through the addition of a constitutive form of calmodulin kinase 2 (CamK2) (Lorca et al., 1993). We monitored the meiotic state by measuring the phosphorylation of mitotic substrates, such as endogenous Gwl (xGwl), Cdc27, Cdc25 (specifically Cdc25c) and MAPK (Erk; also known as Mapk1), as well as the degradation of cyclin B (here, *Xenopus* cyclin B2 was examined) and the decrease of cyclin-B–Cdk1 kinase activity. An antibody against Fcp1 completely depleted Fcp1 from CSF extracts (Fig. 1A). As expected, addition of CamK2 promoted meiotic exit in control extracts (Fig. 1A, ΔCT+ CamK2), as shown by the dephosphorylation of xGwl, Cdc27, Cdc25 and Erk, and by the degradation of cyclin B which coincided with a decrease in cyclin-B–Cdk1 kinase activity (as monitored by phosphorylation of the substrate histone 1; H1K). Unexpectedly, we

[1]Université de Montpellier, Centre de Recherche de Biochimie Macromoléculaire, CNRS UMR 5237, 1919 Route de Mende, Montpellier 34293, Cedex 5, France. Equipe Labellisée 'Ligue Contre le Cancer'. [2]Laboratoire de Spectrométrie de Masse Bio-Organique, Institut Pluridisciplinaire Hubert Curien, UMR 7178, 25 rue Becquerel, Strasbourg F67087, Cedex 2, France.
*These authors contributed equally to this work

‡Authors for correspondence (anna.castro@crbm.cnrs.fr; thierry.lorca@crbm.cnrs.fr)

**Received 10 August 2015; Accepted 12 February 2016**

Journal of Cell Science (2016) 129, 1329-1339 doi:10.1242/jcs.178855

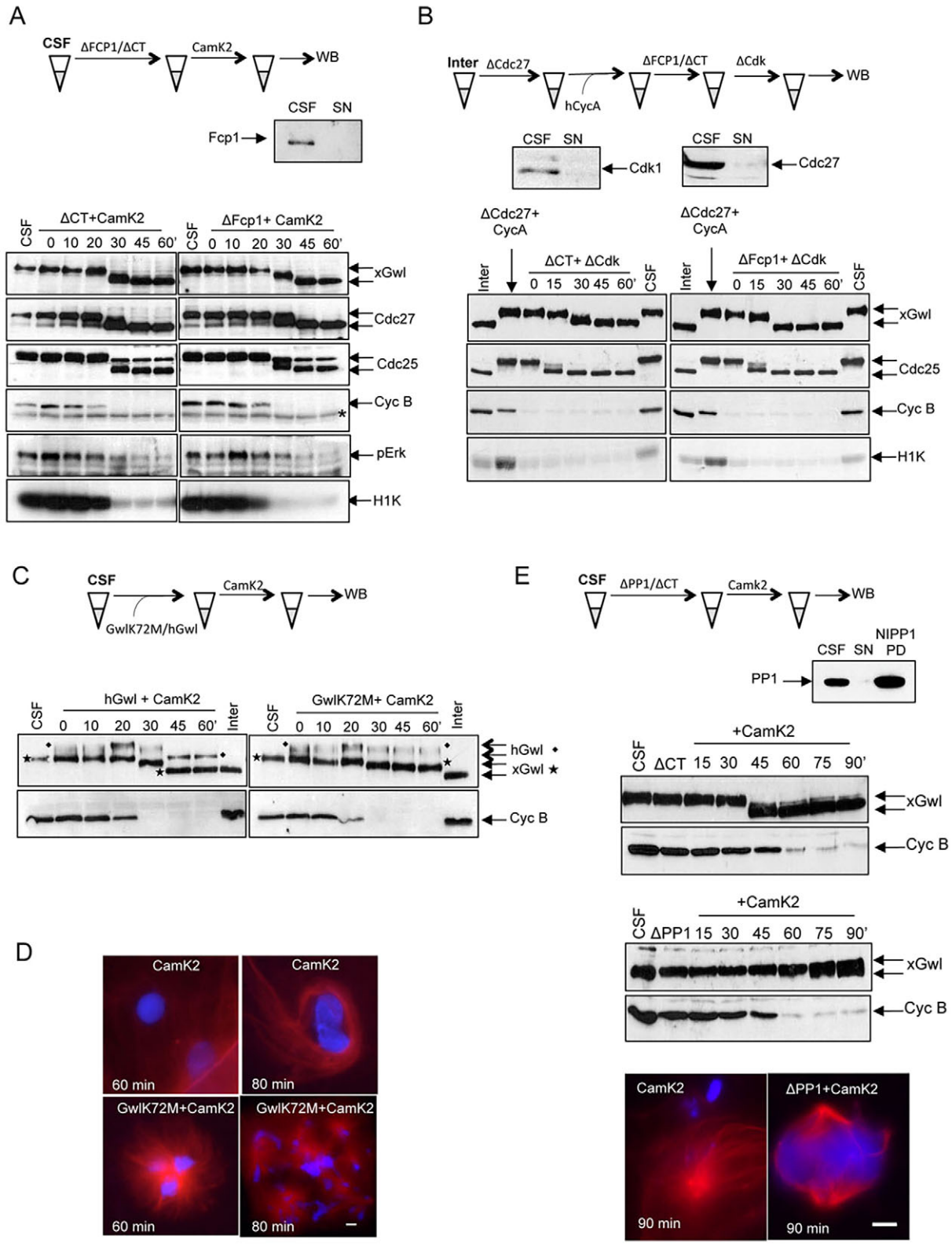


**Fig. 1.** See next page for legend.

did not observe any change in the timing of the dephosphorylation of these proteins when Fcp1 was depleted (Fig. 1A, ΔFcp1+ CamK2), suggesting that Fcp1 is not required to induce meiotic exit in *Xenopus* egg extracts. We next investigated whether this was also the case for mitotic exit. With this aim, we used interphase egg extracts. The addition of ectopic cyclin A (human cyclin A2) to these extracts promotes an increase of cyclin-B–Cdk1 activity, mitotic entry and a subsequent activation of the APC/C, resulting in a rapid exit from mitosis, making it difficult to study the dephosphorylation timing of mitotic substrates. In order to

Journal of Cell Science (2016) 129, 1329-1339 doi:10.1242/jcs.178855

**Fig. 1. PP2A-B55 and PP1, but not Fcp1, are required for correct meiotic exit.** (A) CSF extracts were first used for immunodepletion with control (ΔCT) or anti-Fcp1 antibodies (ΔFcp1), and subsequently forced to exit meiosis by CamK2 addition. Immunodepletion efficacy of Fcp1 antibodies is shown by western blotting (WB) of CSF extracts and supernatants (SN). Dephosphorylation of endogenous Gwl (xGwl), Cdc27 and Cdc25 was determined by western blotting at the indicated times after CamK2 addition by changes in the mobility shift of these proteins (unphosphorylated proteins migrate more quickly). Phosphorylation of MAPK (also known as Mapk1) was checked by using anti-phospho-Erk antibodies (pErk). Cyclin B (Cyc B) degradation and cyclin-B–Cdk1 activity (H1K) are also shown. (B) Interphase extracts were immunodepleted of Cdc27, and mitotic entry was then induced by the addition of human cyclin A (30 nM final concentration). After 40 min, a sample of this extract was recovered to check substrate phosphorylation (ΔCdc27+CycA). Extracts were then first depleted with control antibody or an anti-Fcp1 antibody, and subsequently depleted of Cdks (ΔCdk) activity by immunodepletion. Samples were recovered at the indicated timepoints, and the phosphorylation of endogenous Gwl (xGwl) and Cdc25, as well as the levels of cyclin B and the activity of cyclin-B–Cdk1, were examined. Efficacy of immunodepletion with antibodies against Cdc27 and Cdk1 is shown. (C) CSF extracts were supplemented with the wild-type (hGwl) or the K72M mutant form of human Gwl (GwlK72M) (0.1 µg in 10 µl of CSF extracts), and mitotic exit was then promoted by CamK2 addition. The levels of phosphorylation of endogenous (xGwl) and ectopic (hGwl) Gwl proteins, and the stability of cyclin B, were assessed by western blot. The amount of endogenous cyclin B and xGwl from 1 µl of an interphase egg extract prepared 40 min after ionophore addition in shown. (D) Sperm nuclei and tubulin–Rhodamine were added to CSF extracts that had been supplemented or not with GwlK72M. After 60 min, a constitutive form of CamK2 was added to promote CSF exit. After fixation of the samples (60 and 80 min after CamK2 addition) with 1% formaldehyde containing DAPI (1 µg/ml), a 1 µl sample was used to visualise chromatin condensation and spindle formation with light microscopy. Scale bar: 15 µm. (E) CSF extracts were depleted (ΔPP1) or not of PP1 and supplemented with CamK2 in order to induce mitotic exit. Samples were removed at the indicated times, and Gwl phosphorylation and cyclin B degradation were monitored by western blotting. PP1 or control depletions were obtained by using a pulldown approach in CSF extracts that had been supplemented with a control $His_6$-tagged protein or a $His_6$-tagged protein containing the PP1-binding site of NIPP1 (NIPP1 PD). Efficacy of PP1 depletion is shown. Spindle formation and chromatin condensation in PP1-devoid extracts were observed by microscopy, as indicated in D, except that control depletion or depletion of PP1 instead of GwlK72M addition was performed. Scale bars: 10 µm. Inter, interphase egg extracts.

stabilise mitosis before mitotic exit, we prevented cyclin A and cyclin B degradation by depleting the APC/C subunit Cdc27 (Lorca et al., 2010). After Cdc27 loss, cyclin A was added to promote mitotic entry. After 30 min, H1K activity increased, and the mitotic substrates Cdc25 and xGwl became phosphorylated (Fig. 1B, ΔCdc27+CycA). At this point, Fcp1 was immunodepleted, and mitotic exit was induced by depletion of Cdks. In both control and Fcp1-depleted extracts, Cdk depletion promoted dephosphorylation of xGwl and Cdc25 with similar kinetics, indicating that Fcp1 is not involved in mitotic exit either.

As for Fcp1, PP2A-B55 has been suggested to mediate mitotic exit in human cells by either promoting the dephosphorylation of Gwl on the T-loop activating site (Hégarat et al., 2014), or by inducing the dephosphorylation of cyclin-B–Cdk1 substrates such as PRC1 (Cundell et al., 2013). We tested whether PP2A-B55 is involved in dephosphorylation of Gwl and meiotic exit by investigating the effect of the addition of a human hyperactive mutant form of Gwl (GwlK72M). As wild-type Gwl, this mutant form is able to inhibit PP2A-B55 through Arpp19 phosphorylation but to a much greater extent owing to its increased kinase activity (Fig. S1). In addition, GwlK72M is inactivated by dephosphorylation when cyclin-B–Cdk1 activity reduces in meiosis-exiting egg extracts when this mutant is supplemented at trace levels (Vigneron et al., 2011). We first added equivalent amounts of GwlK72M or wild-type Gwl proteins to CSF extracts and then forced meiotic exit through CamK2 addition. Under these conditions, we assessed cyclin B degradation and Gwl dephosphorylation by western blotting, and the meiotic state by checking chromatin condensation and spindle formation in these extracts. Because our antibody against *Xenopus* Gwl also partially recognises human Gwl (hGwl), our western blots allowed the visualisation of the dephosphorylation of both endogenous (Fig. 1C, xGwl) and ectopic Gwl (Fig. 1C, hGwl). Addition of CamK2 promoted cyclin B degradation with similar kinetics in control and in hGwl- or Gwlk72M-supplemented extracts (compare cyclin B in ΔCT+ CamK2 samples in Fig. 1A with hGWL+CamK2 or GwlK72M+ CamK2 in Fig. 1C). In addition, hGwl-supplemented extracts displayed a similar dephosphorylation pattern of xGwl and hGwl, with identical timing profiles to those of non-supplemented extracts (compare xGwl in Fig. 1A with xGwl and hGwl in Fig. 1C). However, in GwlK72M-supplemented extracts, we observed only a partial dephosphorylation of both the endogenous and ectopic Gwl proteins (Fig. 1C). Incomplete dephosphorylation of Gwl was associated with the maintenance of a partial meiotic state in GwlK72M-supplemented extracts, as shown by the fact that 80 min after CamK2 addition, chromatin was partially condensed and located on short mitotic-like microtubule structures, however, structured bipolar spindles with a metaphase plate was never observed (Fig. 1D). Thus, preventing normal PP2A-B55 reactivation impedes complete meiotic exit but allows the partial dephosphorylation of Gwl, suggesting that other phosphatase(s) could be involved in Gwl dephosphorylation and inactivation upon meiotic exit.

One candidate phosphatase could be PP1 because it has been previously shown that it is required to promote correct mitotic exit in *Xenopus* egg extracts (Wu et al., 2009). We thus checked the effects of PP1 depletion from CSF extracts prior to inducing meiotic exit. In order to remove PP1, we used a His-pulldown approach from CSF extracts in which a His-tagged form of the PP1-binding domain of the PP1 inhibitor NIPP1 (also known as PPP1R8) (Winkler et al., 2015), or a control protein, was added. This pull down efficiently depleted PP1 from the extract (Fig. 1E). The loss of PP1 stabilised Gwl in its phosphorylated form as late as 90 min after CamK2 addition, long after degradation of cyclin B, suggesting that this phosphatase, directly or indirectly, controls the dephosphorylation of Gwl. In addition, extracts devoid of PP1 displayed a clear mitotic state with bipolar spindles and metaphase plates, suggesting that this phosphatase is required to promote Gwl dephosphorylation and meiotic exit.

### Preventing PP2A-B55 reactivation upon meiotic and mitotic exit promotes a significant delay in dephosphorylation of Gwl on Thr194

In order to further characterise the effects of PP2A-B55 on Gwl dephosphorylation and inactivation, we assessed dephosphorylation of this kinase on the two essential activating sites, the T-loop residue Thr193 (Thr194 in human Gwl) and the C-terminal residue Ser883 (Ser875 in the human protein). Under normal conditions, we observed a simultaneous dephosphorylation of hGwl on Ser875 and Thr194 upon meiotic exit, starting at 15 min and completely lost at 30 min (Fig. 2A). As expected, Gwl dephosphorylation was concomitant with cyclin B degradation and with the reactivation of PP1, as revealed by the dephosphorylation of the cyclin-B–Cdk1 inhibitory site Thr320 on this protein (Wu et al., 2009). We next checked the dephosphorylation of these two sites when PP2A-B55 reactivation was prevented by the addition of the GwlK72M hyperactive kinase. The addition of hyperactive Gwl resulted in delayed dephosphorylation of both Ser875 and Thr194 Gwl sites compared with that under control conditions (Fig. 2B, GwlK72M

Journal of Cell Science (2016) 129, 1329-1339 doi:10.1242/jcs.178855

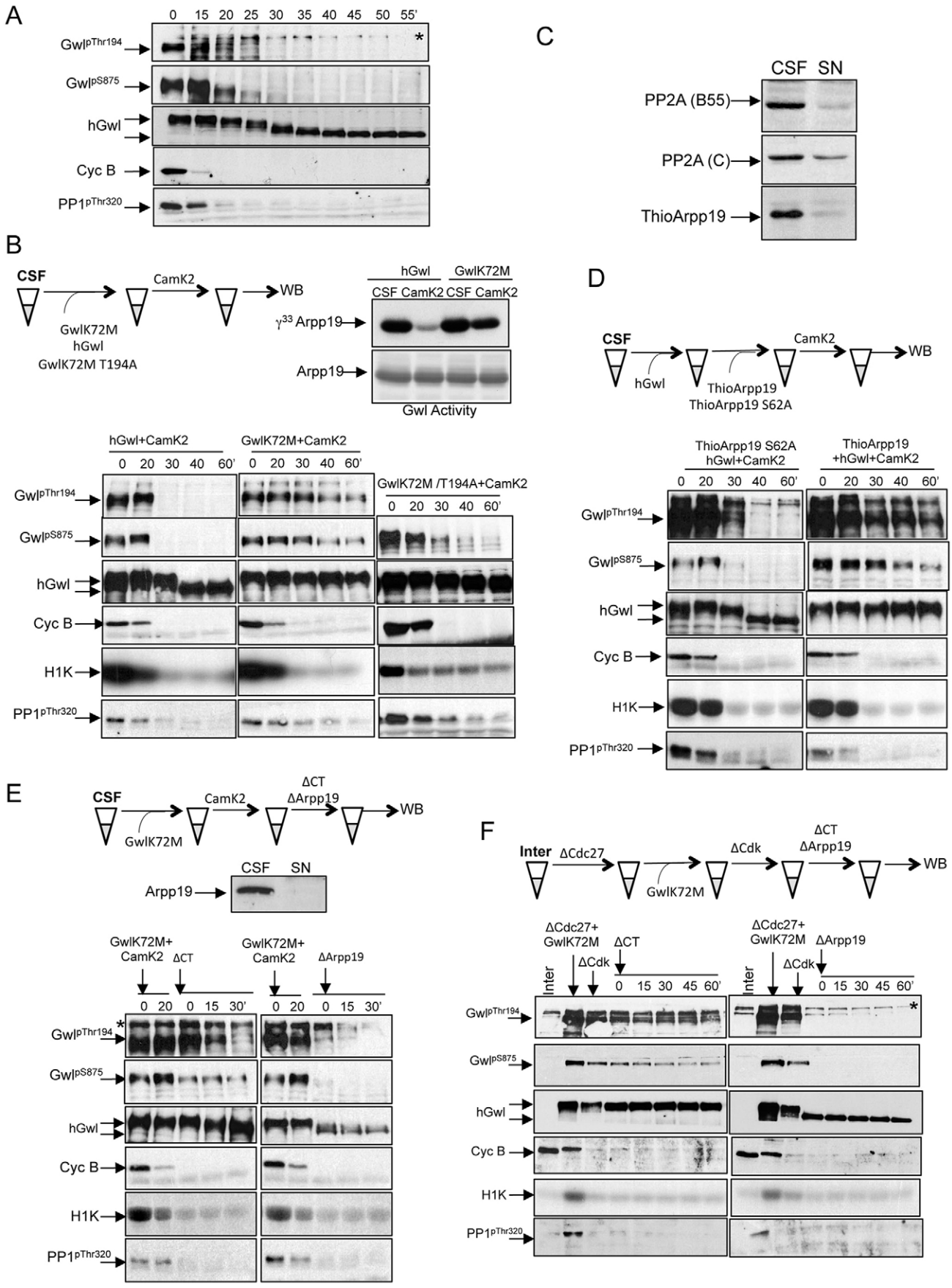


**Fig. 2.** See next page for legend.

Journal of Cell Science (2016) 129, 1329-1339 doi:10.1242/jcs.178855

**Fig. 2. Preventing PP2A-B55 reactivation upon meiotic and mitotic exit promotes a substantial delay of the phosphorylation of Gwl on Thr194.** (A) 20 µl of CSF extracts were supplemented with wild-type Gwl recombinant kinase (hGwl; 1 µg). After 20 min, extracts were supplemented with CamK2, and samples were recovered at the indicated timepoints to study the dephosphorylation of Gwl on Ser875 ($Gwl^{pSer875}$) and Thr194 ($Gwl^{pThr194}$) with phospho-specific antibodies. Cyclin B (cyc B) stability, phosphorylation of PP1 on Thr320 ($PP1^{pThr320}$) and levels of the ectopic human Gwl forms (hGwl) are also shown. (B) 20 µl of CSF extracts were supplemented with either wild-type (hGwl) or GwlK72M recombinant proteins (1 µg), or with 5 µl of CSF extracts in which the mRNA of the GwlK72M T194A double mutant had been translated. After CamK2 addition, samples were taken to check dephosphorylation of Gwl on Ser875 and Thr194, cyclin B stability, cyclin-B–Cdk1 activity, phosphorylation of PP1 on Thr320 and the levels of the ectopic human Gwl. The activity of ectopic human Gwl ($\gamma^{33}$Arpp19) was measured as indicated in Materials and Methods in CSF extracts that had been supplemented with hGwl or GwlK72M 60 min after CamK2 addition. (C) 2 µg of Thio-phosphorylated His–Arpp19 was added to 20 µl of CSF extracts and, after 20 min of incubation, ThioArpp19 was recovered by His-tag pull down. The levels of Arpp19 (ThioArpp19) and the PP2A B55 [PP2A (B55)] and C [PP2A(C)] subunits left in the supernatant were assessed by western blotting (WB). SN, supernatant. (D) The experiment described in A except that Thio-phosphorylated His–Arpp19 (2 µg for 20 µl of CSF extracts) instead of GwlK72M was added. (E) CSF extracts were supplemented with GwlK72M and CamK2, and submitted to a control depletion (ΔCT) or depletion of Arpp19 (ΔArpp19). Phosphorylation of the indicated residues of Gwl was analysed, as well as the ectopic Gwl levels, cyclin B degradation and cyclin-B–Cdk1 activity (H1K). Efficacy of Arpp19 depletion is shown. (F) Interphase extracts were devoid of Cdc27 (ΔCdc17; by immunodepletion) and induced to enter into mitosis by GwlK72M addition. After 40 min, extracts were first forced to exit mitosis by Cdk1 depletion and were subsequently depleted of Arpp19 (or not) by immunoprecipitation. Phosphorylation on Ser875 and Thr194 of Gwl, and on Thr320 of PP1, as well as ectopic GwlK72M and cyclin B levels and cyclin-B–Cdk1 activity are shown. Asterisks denote non-specific bands recognised by the antibodies. Inter, interphase.

+CamK2 and hGwl+CamK2). Gwl, in which Ser875 and Thr194 had been partially dephosphorylated, displayed an intermediate activity between that observed in CSF extracts and that observed in interphase extracts (Fig. 2B, Gwl Activity). It is known that Ser875 phosphorylation is the result of autophosphorylation and that this relies on prior phosphorylation on Thr194. Consequently, intermediate phosphorylation levels of Gwl on Ser875 could be the result of either decreased dephosphorylation of this site or maintained autophosphorylation activity owing to delayed dephosphorylation of Thr194. To test this hypothesis, we repeated the experiment by supplying CSF extracts with a double GwlK72M and T194A mutant form of Gwl. As shown in Fig. 2B, residue Ser875 of the GwlK72M T194A double mutant became phosphorylated in CSF extracts, indicating that this site was probably intermolecularly phosphorylated by endogenous xGwl. Interestingly, after CamK2 addition, Ser875 was completely dephosphorylated with similar kinetics to that of wild-type hGwl protein. These data indicate that the remnant phosphorylation of Thr194 observed in GwlK72M-supplemented extracts is the result of decreased PP2A-B55-dependent dephosphorylation of this site. In addition, they also indicate that the residual phosphorylation on Ser875 is not due to a decreased dephosphorylation of this residue as a result of PP2A-B55 inhibition but to maintained autophosphorylation.

To confirm these results, we repeated the previously described experiment by preventing reactivation of PP2A-B55 using thio-phosphorylated wild-type Arpp19 (ThioArpp19) or an inactive Arpp19 mutant form as a control (ThioArpp19S62A). We chose an amount of Arpp19 that, when immunoprecipitated from the extracts, induced an efficient loss of PP2A-B55 from the supernatants (Fig. 2C). Upon CamK2 addition, ThioArpp19-supplemented CSF extracts exhibited substantially delayed dephosphorylation of residue Ser875 and almost completely stabilised phosphorylation of Gwl on Thr194, despite the fact that cyclin B degradation was complete and that cyclin-B–Cdk1 activity had been completely inhibited (Fig. 2D). It is worth noting that PP1 is normally dephosphorylated on Thr320 and is, thus, reactivated in these extracts concomitant with the loss of cyclin-B–Cdk1 activity.

To further check whether the effect of GwlK72M addition on dephosphorylation of the two Gwl activating sites is the consequence of an impaired reactivation of PP2A-B55, we measured the dephosphorylation of the activating sites in GwlK72M-supplemented extracts, in which PP2A-B55 is rapidly reactivated by the depletion of Arpp19 after CamK2 addition. Arpp19 loss promoted a fast and complete dephosphorylation of both Gwl sites (Fig. 2E, ΔArpp19), indicating that in the presence of active PP1, a gradual reactivation of PP2A-B55 is required for the correct timing of Gwl inactivation and meiotic exit.

We next checked whether the role of PP2A-B55 upon exit of meiosis is also conserved during mitotic exit. To that end, we supplemented Cdc27-devoid interphase extracts with GwlK72M, which directly promoted mitotic entry (Fig. 2F), and we subsequently depleted Cdks to promote mitotic exit. Again, the impaired reactivation of PP2A-B55 through hyperactivation of GwlK72M promoted partial dephosphorylation of Gwl on Ser875 after depletion of Cdks, whereas in this case, phosphorylation of Thr194 was almost completely stabilised, despite the loss of cyclin B, a drop in cyclin-B–Cdk1 activity and a reactivation of PP1. As for meiotic exit, depletion of Arpp19 promoted an immediate dephosphorylation of both activating sites of Gwl. Altogether, these results indicate that during normal mitotic and meiotic exit, PP2A-B55 is the phosphatase that is mostly responsible for the dephosphorylation of Gwl on Thr194; however, we cannot exclude the possibility that it could also, to a minor extent, contribute directly or indirectly to the dephosphorylation of Gwl on Ser875. In addition, we show that if the rapid reactivation of PP2A-B55 is artificially induced by Arpp19 immunodepletion, this phosphatase is able to immediately dephosphorylate both activating sites on Gwl.

### PP1 depletion prevents Gwl inactivation upon meiotic and mitotic exit by maintaining phosphorylation on residue Ser875

Our data above suggest that, besides PP2A-B55, PP1 activity is also required for Gwl dephosphorylation and inactivation, because its depletion maintains this kinase in its phosphorylated form upon meiotic exit (Fig. 1E). To further identify whether PP1 targets the sites of Gwl that control its kinase activity, we performed western blot analyses of the phosphorylation of Thr194 and Ser875 in extracts devoid of PP1 upon CamK2 addition. As shown in Fig. 3A, depletion of PP1 in CSF extracts promoted a delay in the dephosphorylation of residue Thr194, but a substantial stabilisation of phosphorylated residue Ser875. Interestingly, phosphorylation of Ser875 was also maintained in the GwlK72M T194A double mutant, indicating that the stabilisation of Ser875 phosphorylation was the result of a decreased dephosphorylation of the Thr194 residue. In addition, under these conditions, Gwl activity was fully maintained, indicating that inactivation of Gwl is mainly promoted by dephosphorylation of Ser875. We could not obtain proof of the specificity of NIPP1-dependent immunodepletion of PP1 by performing add-back experiments, probably owing to the co-depletion of other PP1 regulators required for its activation. However, we obtained the same results when protein phosphatase

Journal of Cell Science (2016) 129, 1329-1339 doi:10.1242/jcs.178855

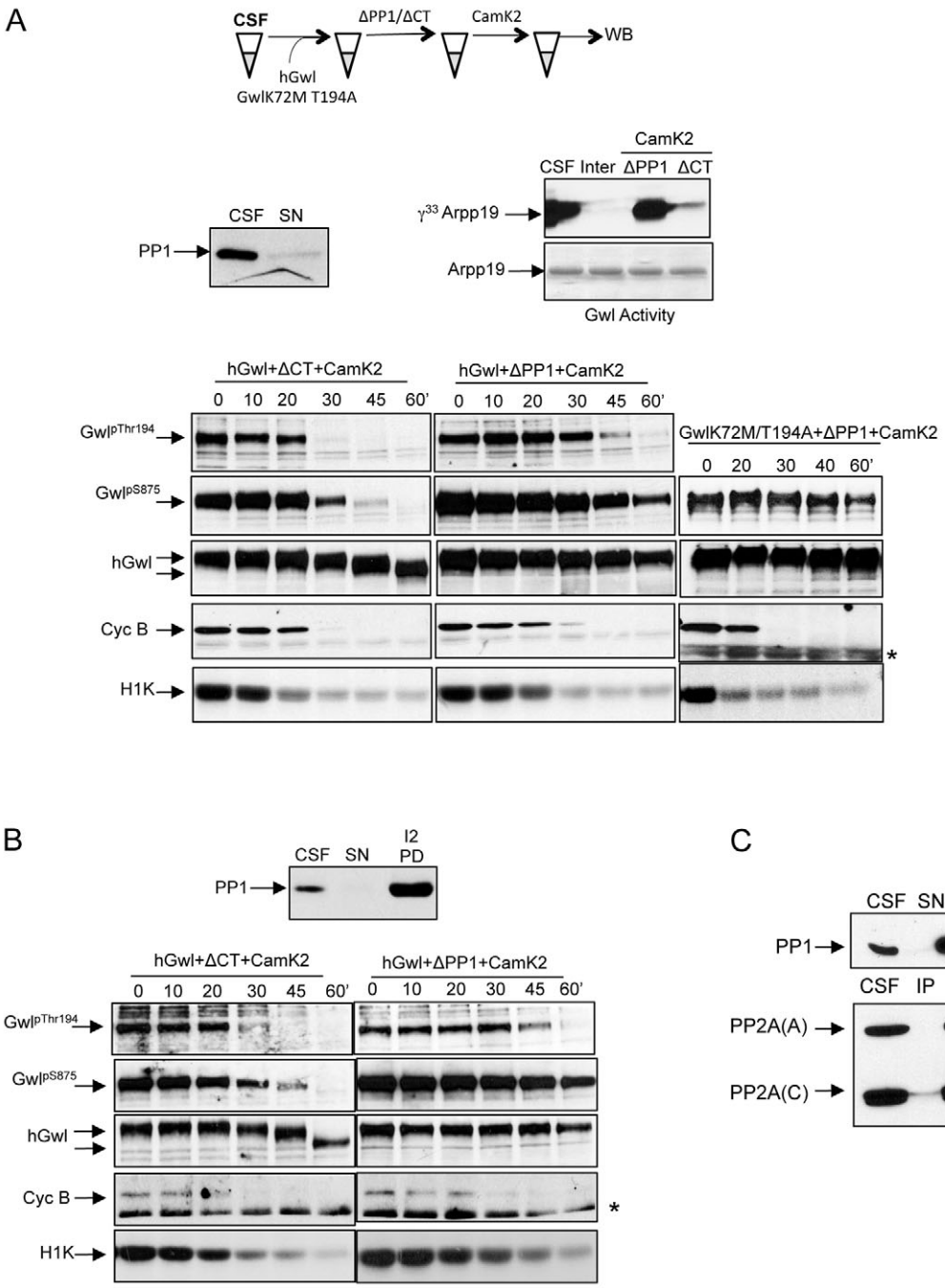


**Fig. 3. PP1 depletion prevents Gwl inactivation upon meiotic exit by maintaining its phosphorylation on Ser875.** (A) CSF extracts supplemented with human wild-type or K72M T194A double mutant (GwlK72M/T194A) forms of Gwl were devoid (ΔPP1) (or not) of PP1 after pull down using $His_6$-tagged NIPP1 or control proteins prior to CamK2 addition, and the phosphorylation of the indicated sites of Gwl, as well as ectopic Gwl levels, cyclin B degradation and cyclin-B–Cdk1 activity, were assessed. Efficacy of PP1 depletion is shown. Activity of human Gwl ($\gamma^{33}$Arpp19) was measured as described in Materials and Methods in CSF and interphase extracts and compared to the level obtained in CSF (depleted or not of PP1) 60 min after CamK2 addition. Time (min) after treatment is shown across the top of the blots. (B) CSF extracts supplemented with human wild-type Gwl were devoid (or not) of PP1 after pull down using inhibitor 2 (I2 PD) or control $His_6$-tagged proteins prior to CamK2 addition, and the phosphorylation of the indicated residues of Gwl, as well as the ectopic Gwl levels, cyclin B degradation and cyclin-B–Cdk1 activity, were assessed. (C) PP1 pull down. The supernatant (SN) and the CSF extracts supplemented with $His_6$–NIPP1-binding domain were assessed for the levels of PP1 and the A and C subunits of PP2A [PP2A(A) and PP2A(C), respectively]. IP, immunoprecipitation; WB, western blotting. Asterisks denote non-specific bands recognised by the antibodies.

inhibitor 2 (I2; also known as PPP1R2) (Satinover et al., 2004), another inhibitor of PP1, was used to perform pull down of PP1 (Fig. 3B).

Thus, our results suggest that the major target site of PP2A-B55 in Gwl is Thr194, whereas PP1 preferentially dephosphorylates Gwl on Ser875, although a minor effect on dephosphorylation at Thr194 cannot be excluded.

We next asked if PP1 directly dephosphorylates Ser875 or whether it is mediated by reactivation of PP2A-B55 that, as shown above, can induce the complete dephosphorylation of this site when

Journal of Cell Science (2016) 129, 1329-1339 doi:10.1242/jcs.178855

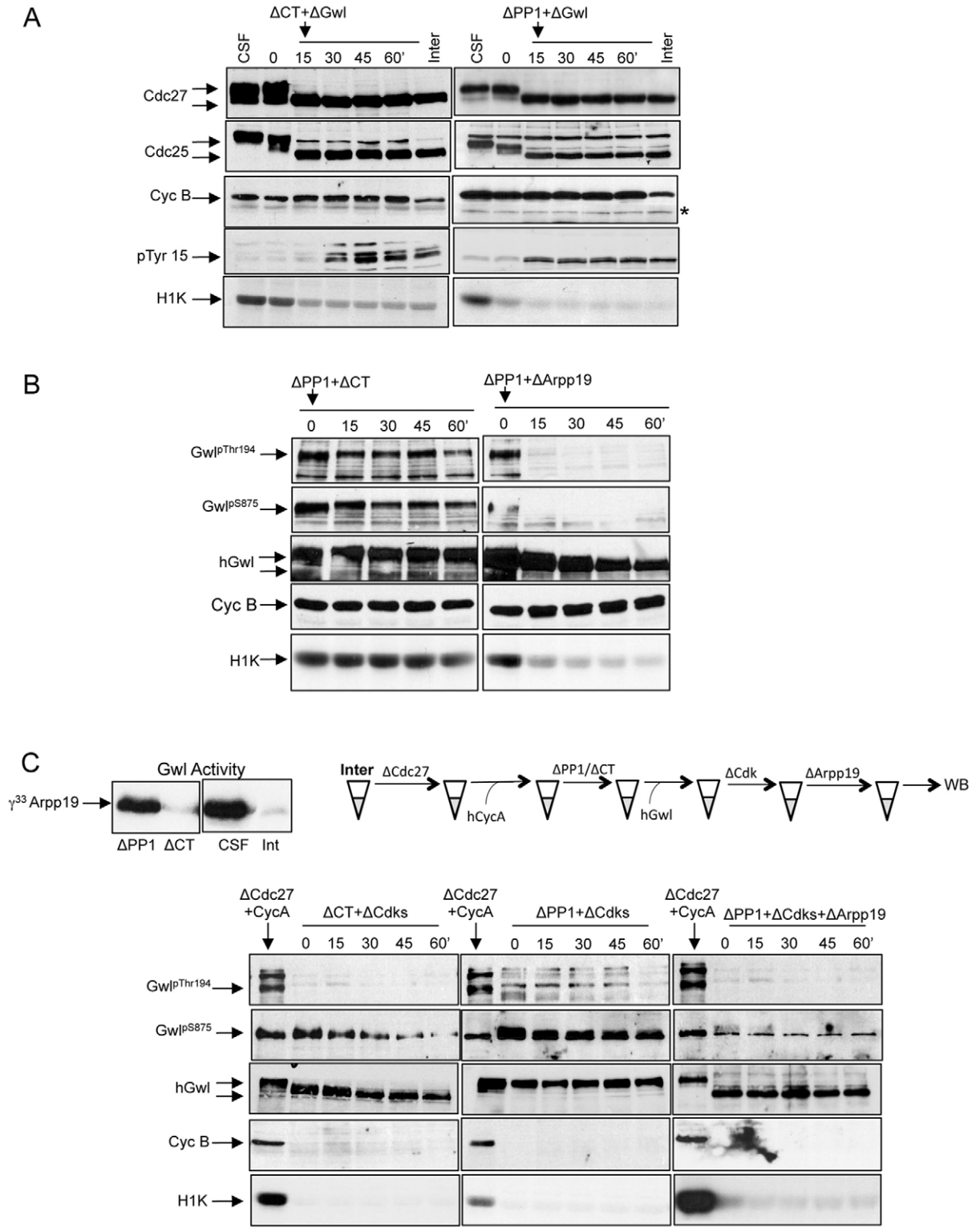


**Fig. 4. PP1 is also involved in dephosphorylation of Ser875 on Gwl upon mitotic exit.** (A) CSF extracts were first immunoprecipitated with anti-PP1 (ΔPP1) antibodies or with control (ΔCT) antibodies, and subsequently depleted of Gwl (ΔGwl). The phosphorylation of Cdc27, Cdc25, Tyr15 of Cdk1 (pTyr 15) and the levels of cyclin B (cyc B) and of H1K activity were monitored by western blotting (WB). (B) CSF extracts were depleted of PP1 and subsequently submitted to a control or Arpp19 (ΔArpp19) depletion. The phosphorylation of the two activating sites of Gwl, as well as the levels of ectopic Gwl, cyclin B and the activity of cyclin-B–Cdk1 (H1K) are shown. (C) Interphase extracts were depleted of Cdc27 and subsequently forced to enter into mitosis by the addition of cyclin A (hCycA). Extracts were then depleted (or not) of PP1, supplemented with hGwl and forced to exit mitosis by immunoprecipitation of Cdks (ΔCdks). Some of the PP1- and Cdk-depleted extract was subsequently depleted of Arpp19, and the phosphorylation on the different residues of Gwl, and the ectopic Gwl levels, cyclin B stability and H1K activity, were measured. hGwl activity was measured in extracts that had been depleted (or not) of PP1 60 min after Cdks immunoprecipitation and was compared to that obtained in CSF and interphase extracts that had been supplemented with the same amount of this ectopic kinase. Asterisks denote non-specific bands recognised by the antibodies. Int, Inter, interphase egg extracts.

Journal of Cell Science (2016) 129, 1329-1339 doi:10.1242/jcs.178855

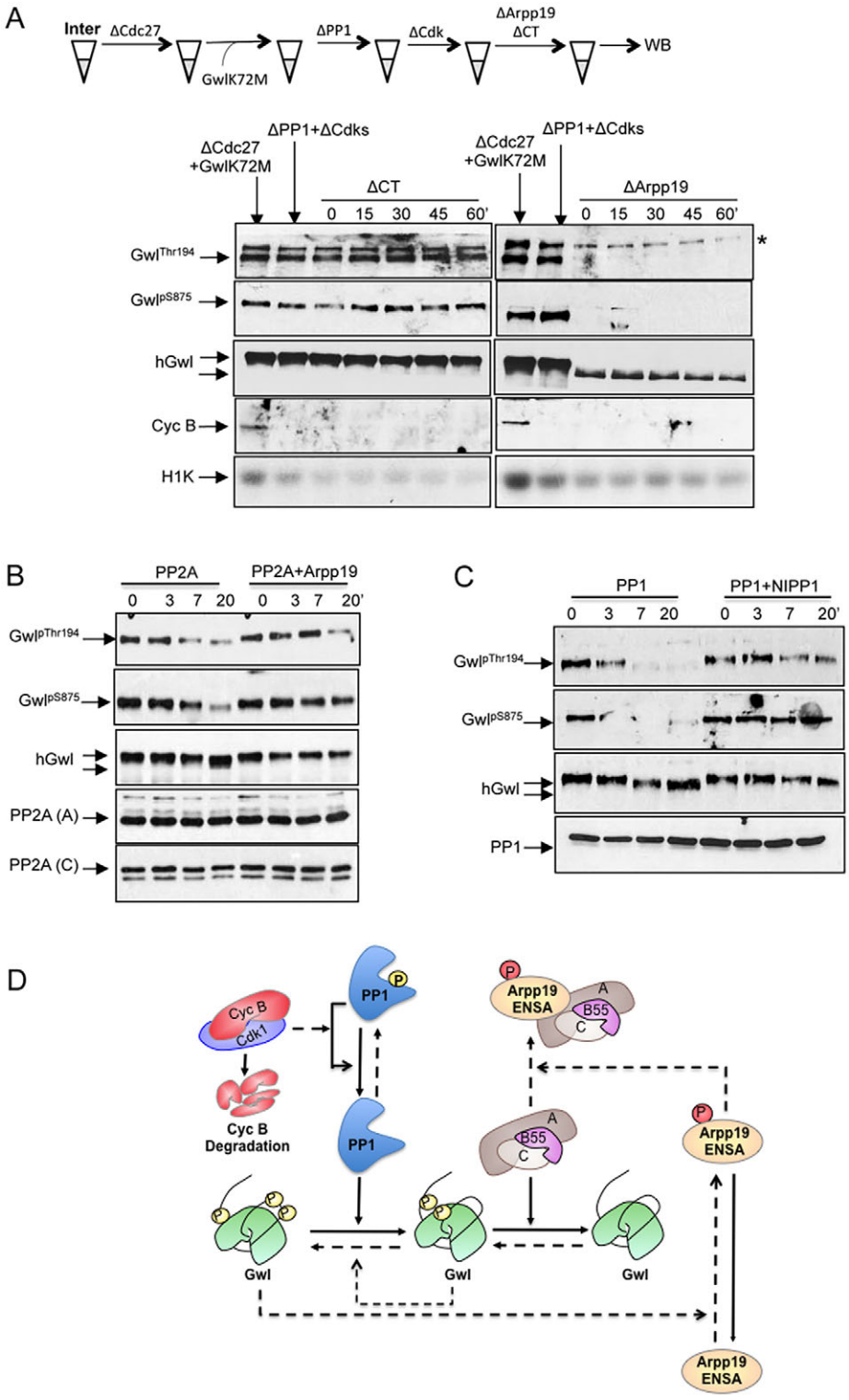


**Fig. 5. PP1 and PP2A-B55 both dephosphorylate Gwl on Thr194 and Ser875 *in vitro*.** (A) Interphase extracts were depleted of Cdc27, supplemented with GwlK72M, depleted of PP1 (ΔPP1) and Cdks (ΔCdks) by immunoprecipitation, and finally depleted (or not) of Arpp19. Phosphorylation of Ser875 and Thr194 of Gwl, as well as ectopic Gwl levels (hGwl), the stability of cyclin B (cyc B) and cyclin-B–Cdk1 activity (H1K) are shown. Asterisks denote non-specific bands recognised by the antibodies. (B) Phosphorylated hGwl and active PP2A were obtained by GST pull down and immunoprecipitation from CSF and interphase extracts, respectively, and incubated together with or without ThioArpp19 at room temperature for a dephosphorylation assay. Samples were recovered at the indicated times (min) and monitored for phosphorylation of Gwl on Ser875 and Thr194. Protein levels of Gwl and the PP2A A [PP2A(A)] and C [PP2A(C)] subunits were also assessed. (C) A dephosphorylation assay was performed as described in B, except that active PP1 was obtained by His pull down from interphase extracts that had been supplemented with ectopic $His_6$–PP1 and the NIPP1 inhibitor instead of ThioArpp19. (D) Working model showing the mechanisms by which cyclin B degradation promotes Gwl inactivation and mitotic exit. Full arrows represents active pathway in mitotic exit; dashed arrows represent inactive pathways in mitotic exit. 'A', PP2A subunit A; B55, B55 subunit of PP2A; 'C', PP2A subunit C; P, phosphate group.

fully reactivated. Given that it has recently been shown in fission yeast that PP1 association with PP2A-B55 during mitosis promotes the activation of PP2A-B55 (Grallert et al., 2015), we tested whether these two phosphatases interact in CSF extracts. We did not detect any association of the PP2A scaffolding A subunit (also known as PPP2R1A) or a PP2A catalytic subunit (PPP2CA) with PP1 in our extracts by performing either western blotting (Fig. 3C) or mass spectrometry analysis (Table S1), suggesting that the loss of an interaction between PP1 and PP2A-B55 is not the mechanism by which PP1 removal prevents Gwl dephosphorylation on Ser875 and meiotic exit in these extracts.

We thus tested if PP1 depletion maintains the meiotic state exclusively by stabilising Ser875 phosphorylation and by preventing, in this way, Gwl inactivation or whether it is also be mediated by the dephosphorylation of other proteins, such as Arpp19. If the sole effect of PP1 depletion is the maintenance of Gwl activity, extracts should exit meiosis when PP1 and Gwl are co-depleted. Accordingly, the double depletion of PP1 and Gwl

Journal of Cell Science (2016) 129, 1329-1339 doi:10.1242/jcs.178855

promoted the rapid dephosphorylation of mitotic substrates. This indicates that, under these conditions, PP2A-B55 is activated and Arpp19 is dephosphorylated, excluding the possibility that PP1 blocks mitotic exit through the dephosphorylation of Arpp19 or other mitotic proteins (Fig. 4A). In addition, depletion of Arpp19 in extracts devoid of PP1 induced a rapid and complete dephosphorylation of Gwl at both the Thr194 and Ser875 sites (Fig. 4B). These results suggest that PP1 is essential for the dephosphorylation of Gwl on Ser875 when App19-dependent inhibition of PP2A-B55 is present but that the latter phosphatase can promote the rapid and complete dephosphorylation of Gwl if the Arpp19 inhibition pathway is shut down.

Finally, we investigated whether the effect of PP1 on Gwl dephosphorylation and inactivation can also be observed during mitotic exit. Therefore, we repeated the PP1 depletion experiment in interphase egg extracts that had been forced to enter into mitosis through cyclin A addition and to exit mitosis through depletion of Cdks. Again, phosphorylation of residue Ser875 of Gwl was stabilised, and the activity of this kinase was fully maintained (Fig. 4C). As during meiotic exit, this modification was mediated by the maintenance of Gwl activity and the inhibition of PP2A-B55 by Arpp19 because, when Arpp19 was depleted after immunoprecipitation of Cdks, Gwl was completely dephosphorylated on Ser875.

### The double inhibition of PP2A-B55 and PP1 completely blocks dephosphorylation of Gwl on both Thr194 and Ser875

Our data is consistent with a model in which PP1 first triggers dephosphorylation of residue Ser875, allowing partial activation of PP2A-B55. PP2A-B55 then takes over Gwl dephosphorylation by preferentially dephosphorylating Thr194. However, it is possible that other phosphatases can also contribute to these dephosphorylation events. If PP2A-B55 and PP1 are the only phosphatases involved in dephosphorylation of activating Gwl sites, the double inhibition of PP2A-B55 and PP1 should completely prevent dephosphorylation of these two sites upon mitotic exit. To test this hypothesis, we used interphase extracts that were first forced to enter into mitosis by GwlK72M addition, then depleted of PP1 and finally forced to exit mitosis by depletion of Cdks. As shown in Fig. 5A, the loss of the activities of PP2A-B55 and PP1 completely prevented dephosphorylation of Gwl on Thr194 and Ser875. However, PP1 was only essential for Gwl inactivation when PP2A-B55 was inhibited by Arpp19 because, in the absence of this phosphatase inhibitor, Gwl was fully dephosphorylated by PP2A-B55.

### PP1 and PP2A-B55 both dephosphorylate Gwl on Thr194 and Ser875 *in vitro*

In order to determine whether PP1 and PP2A-B55 can directly promote dephosphorylation on Thr194 and/or Ser875 of Gwl, we performed *in vitro* dephosphorylation assays on phosphorylated Gwl by using PP2A and PP1 phosphatases that had been purified from interphase extracts. As shown in Fig. 5B, dephosphorylation of Gwl on both Ser875 and Thr194 was observed after 7 min of incubation, and promoted an increase in the dephosphorylated forms of this kinase 20 min after PP2A addition. This dephosphorylation was significantly delayed when Arpp19 was supplemented into the incubation buffer, suggesting that PP2A-B55 contributes to this dephosphorylation. As for PP2A, PP1 promoted the dephosphorylation of these two phosphorylation sites of Gwl, which was prevented by the addition of the PP1 inhibitor NIPP1. These results suggest that, *in vitro*, both PP1 and PP2A-B55 can induce dephosphorylation of Gwl on residues Ser875 and Thr194.

## DISCUSSION

Our data presented here demonstrate that both PP1 and PP2A-B55 participate in the dephosphorylation of Gwl on its activating sites during meiotic and mitotic exit. This dephosphorylation induces Gwl inactivation and is likely to promote the further dephosphorylation of Arpp19 and ENSA, and the reactivation of PP2A-B55 that is required to induce dephosphorylation of mitotic substrates and meiotic and mitotic exit. Although both PP2A-B55 and PP1 promote dephosphorylation of both Ser875 and Thr194 of Gwl *in vitro*, our results suggest that, *in vivo*, each phosphatase preferentially dephosphorylates one of these two sites. In this regard, we show that the inhibition of PP2A-B55 by the addition of GwlK72M or ThioArpp19 upon meiotic or mitotic exit promotes a substantial stabilisation of the phosphorylation of Gwl on Thr194 and only a delay in the dephosphorylation of Ser875, which results from the persistent autophosphorylation activity of Gwl phosphorylated on Thr194.

Unlike PP2A-B55 inhibition, removal of PP1 promotes the stabilisation of phosphorylated Ser875, whereas dephosphorylation of Thr194 is delayed but complete at the end of the experiment. Gwl with dephosphorylated Thr194 residues still has a high level of kinase activity, suggesting that this kinase is still able to maintain Arpp19-dependent inhibition of PP2A-B55. However, under these conditions, PP2A-B55 might be still active at a basal level that is sufficient to promote Thr194 dephosphorylation in the absence of cyclin-B–Cdk1 activity because this dephosphorylation is completely blocked when double inhibition of PP1 and PP2A-B55 is performed. Interestingly, although dephosphorylation of Thr194 on Gwl is complete, PP1-devoid extracts cannot exit mitosis because we observed that DNA is maintained in a condensed form on bipolar spindles that form metaphase plates. Thus, Gwl dephosphorylation on Ser875 induced by PP1 would be essential to trigger partial reactivation of PP2A-B55 that, at this low-level phosphatase activity, would preferentially dephosphorylate Thr194, promoting its partial reactivation. As soon as PP2A-B55 reaches a threshold activity level, it is likely to contribute to both Thr194 and Ser875 dephosphorylation, resulting in the complete reactivation of PP2A-B55 and a rapid dephosphorylation of mitotic substrates.

Interestingly, when PP1-devoid extracts were depleted of Arpp19, PP2A-B55 was rapidly and completely reactivated, resulting in an almost immediate mitotic or meiotic exit. These results suggest that a gradual inactivation of Gwl by PP1-mediated dephosphorylation, resulting in a gradual reactivation of PP2A-B55, is essential to promote a correct timing of mitotic exit.

We propose a model in which the first step of meiotic or mitotic exit is cyclin B proteolysis and subsequent cyclin-B–Cdk1 inactivation (Fig. 5D). Degradation of cyclin B induced by APC/C activation at meiotic or mitotic exit prevents the further phosphorylation of the inhibitory site of PP1 on Thr320, allowing the reactivation of this phosphatase through autodephosphorylation. Once activated, PP1 first triggers the inactivation of Gwl by dephosphorylating the Ser875 activating site. This induces a partial dephosphorylation of Arpp19 and ENSA, a partial reactivation of PP2A-B55 and a further dephosphorylation by the latter phosphatase of Gwl preferentially on Thr194 but also on Ser875. Full dephosphorylation of Gwl then results in complete inactivation of Arpp19 and ENSA, and dephosphorylation of mitotic substrates. Once triggered by PP1, this feed-back loop irreversibly induces mitotic exit.

Journal of Cell Science (2016) 129, 1329-1339 doi:10.1242/jcs.178855

## MATERIALS AND METHODS

### CSF and interphase *Xenopus* egg extracts

CSF and interphase *Xenopus* egg extracts were prepared as described previously in Lorca et al. (2010). The care and use of animals was approved by the Direction Départementale de la Protection des Populations (authorization number A34-172-39).

### Mitotic spindle formation and chromatin condensation in extracts

De-membraned sperm nuclei were prepared as described previously (Vigneron et al., 2004). Fresh CSF extracts were supplemented with sperm nuclei and Rhodamine–tubulin to a final concentration of 3000 sperm nuclei per microliter and 22 ng/µl, respectively, and incubated for 30 min at room temperature. Then, 2 µl of constitutive CamK2 translated in reticulocyte lysate was added, and samples were taken at the indicated times and fixed in a buffer containing 1% formaldehyde with DAPI (1 µg/ml) and analysed using light microscopy.

### Light microscopy

A DMR A Leica microscope DM 4500B with a 63× immersion oil objective (HCX PL APO) tube factor 1 was used for epifluorescence imaging. Images were captured with a CoolSnap HQ camera (Roger Scientific), and the whole set was driven by MetaMorph (Universal Imaging, Downingtown, PA).

### Histone 1 kinase activity

H1K activity was analysed as described previously in Lorca et al. (2010).

### Gwl kinase assays

Human GST–Gwl or GST–GwlK72M was added to CSF or interphase extracts to a final concentration of 10 ng/µl. A sample of 10 µl of the mix was recovered 30 min later or at the end of the experiment and mixed with 10 µl of magnetic protein-G-Dynabeads (Dynal) pre-bound to 2 µg of anti-GST antibody. Beads were then incubated for 20 min, recovered and washed with XB buffer (100 mM KCl, 0.1 mM $CaCl_2$, 1 mM $MgCl_2$, 50 mM sucrose). Immunoprecipitate was then mixed with 10 µl of phosphorylation mix (20 µM HEPES, 10 mM $MgCl_2$, 100 µM ATP), 1 µg of His–Arpp19 and 2 µCi of [$\gamma$-$^{33}$P]ATP. After 20 min, reactions were stopped by adding Laemmli sample buffer and were analyzed by performing SDS-PAGE.

### Immunoprecipitations and immunodepletions

Immunoprecipitations and immunodepletions were performed using 10 µl of extracts, 10 µl of magnetic protein-G-Dynabeads (Dynal) and 2 µg of each antibody. Antibody-linked beads were washed twice with XB buffer, twice with 50 mM Tris-HCl, pH 7.5, and incubated for 15 min at room temperature with 10 µl of *Xenopus* egg extracts. For immunodepletion, the supernatant was recovered and used for subsequent experiments.

To induce complete Cdk depletion, two rounds of immunoprecipitation, one with anti-Cdk1 antibody and the second one with anti-cyclin-A antibody (cyclin A binds to Cdk2; thus, this reaction also depletes Cdk2), were performed.

### PP1 depletion

To induce PP1 depletion, 10 µl of CSF or interphase extracts were supplemented with 10 µl of Dynabeads His-Tag Isolation & Pulldown beads (Life Technologies), pre-linked to a control protein ($His_6$-tagged HMGA2) or $His_6$-tagged proteins containing the PP1-binding domain of NIPP1 (amino acids 143–225 of the human NIPP1 sequence). After a 20 min incubation, the supernatant was recovered and used as indicated in each experiment. When indicated, PP1 was immunodepleted by using $His_6$-tagged *Xenopus* I2 instead of the $His_6$-tagged PP1-binding domain of NIPP1.

### *In vitro* phosphatase assay

To obtain active PP2A phosphatase, 150 µl of interphase egg extracts were subjected to immunoprecipitation with 10 µl of a monoclonal antibody recognising the C subunit of PP2A (clone 1D6) bound to 50 µl of Dynabeads protein-G magnetic beads. The immunoprecipitate was then split into two. One half was supplemented with 3 µg of *Xenopus* Thio-phosphorylated Arpp19, whereas the other was mixed with the same volume of the dephosphorylation buffer (50 mM Hepes, 20 mM NaCl, 5 mM $MgCl_2$).

To obtain active PP1 phosphatase, 150 µl of interphase egg extracts was supplemented with 50 µl of Dynabeads His-Tag Isolation & Pulldown beads (Life Technologies) that had been pre-saturated with recombinant $His_6$–PP1 protein. After a 30-min incubation, immunoprecipitate was recovered, washed three times with XB buffer and then split into two. One of these samples was supplemented with 3 µg of the $His_6$-tagged peptide-binding domain of NIPP1, whereas the other was mixed with the same volume of the dephosphorylation buffer.

To obtain phosphorylated human Gwl, 30 µg of GST–hGwl was mixed with 140 µl of CSF extracts. After 40 min, 50 µl of magnetic protein-G-Dynabeads (Dynal) that had been pre-bound to 5 µg of anti-GST antibodies were added to immunoprecipitate GST–hGwl. The immunoprecipitate was separated into four samples, and mixed with PP2A and PP1, supplemented or not with Thio-Arpp19 or $His_6$-tagged peptide-binding domain of NIPP1. A sample of 2 µl was removed at 0, 3, 7 and 20 min and used for western blotting.

### Thio-phosphorylation of *Xenopus* Arpp19

30 µl of magnetic protein-G-Dynabeads (Dynal) pre-bound to 3 µg of anti-xGwl antibodies were mixed with 60 µl of CSF extracts and incubated for 30 min. The immunoprecipitate was then washed a first time with 50 mM Tris-HCl pH 7.5 with 300 mM NaCl, a second time with 50 mM Tris-HCl pH 7.5 with 150 mM NaCl and a third time with 50 mM Tris-HCl pH 7.5, and was finally mixed with 90 µl of *Xenopus* Arpp19 (225 µg) and 10 µl of phosphorylation buffer (×10) (250 mM Tris-HCl pH 7.5, 100 mM $MgCl_2$, 0.4 mM ATP$^{\gamma S}$ and ATP 0.1 nM) and incubated for 1 h at room temperature.

### Antibodies and plasmids

Plasmids and antibodies are specified in Tables S2 and S3.

### mRNA translation

mRNAs encoding GwlK72M T194A double mutant and the constitutive form of rat CamK2 comprising amino acids 1–290 were transcribed *in vitro* from pCS2HA-hGwl-K72M-T194A and pCS2-(1-290) rCamK2 plasmids (see Table S3) with the SP6 RNA polymerase. For mRNA translation, CSF egg extracts were supplemented with dithiothreitol (DTT; 1 mM), RNAguard (0.4 U/l extract; Amersham Biosciences), tRNA (0.1 g/l) and the corresponding mRNA (0.05 g/l extract), and incubated for 2 h at 20°C (Vigneron et al., 2004).

### Western blot results

Samples were electrophoresed on SDS-PAGE and electro-transferred to nitrocellulose membrane. Next, western blots were probed with primary antibody and the appropriate secondary antibody. All shown western blots are representative of at least three different experiments.

### Mass spectrometry

I2 pull downs obtained from CSF extracts that had been supplemented with a $His_6$-tagged *Xenopus* I2 protein were subjected to SDS-PAGE analysis. Bands corresponding to proteins with a molecular mass in the range 70 to 25 KDa were excised, submitted to tryptic digestion, extracted and directly analysed by using nano liquid chromatography tandem mass spectrometry (nanoLC-MS/MS). NanoLC-MS/MS was performed using a nanoACQUITY ultra performance liquid chromatography (UPLC®) system (Waters, Milford, MA) coupled to a maXis 4G Q-TOF mass spectrometer (BrukerDaltonics, Bremen, Germany). The system was fully controlled by HyStar 3.2 (BrukerDaltonics). The UPLC system was equipped with a Symmetry C18 precolumn (20×0.18 mm, 5-µm particle size; Waters, Milford, MA) and an ACQUITY UPLC® BEH130 C18 separation column (75 µm×250 mm, 1.7-µm particle size; Waters, Milford, MA). Peak lists in mascot generic format (.mgf) were generated using Data Analysis (version 4.0; Bruker Daltonics, Bremen, Germany).

### MS/MS data interpretation

The peak list was searched against a *Xenopus* (Uniprot) combined target-decoy database (created 2015-07-21, containing 48,380 target sequences plus the same number of reversed decoy sequences) using Mascot (version 2.5.1, Matrix Science, London, England). The database contained sequences of human proteins, including common contaminants (human keratins and porcine trypsin) and was created using an in-house database generation toolbox (http://msda.u-strasbg.fr). During the database search, up to one missed cleavage by trypsin and two variable modifications [oxidation of methionine (+16 Da) and carbamidomethylation of cysteine (+57 Da) residues, were considered]. The search window was set to 10 ppm for precursor ions and 0.02 Da for fragment ions. Mascot result files (.dat) were imported into Scaffold 3 software (version 3.6.5; Proteome Software Inc., Portland, OR) and filtering criteria based on probability-based scoring of the identified peptides were taken into account – peptides having an ion score>minus identity score above 0 and a Mascot Ion score>25 were validated. The retained proteins had to have at least two peptides corresponding to these criteria.

#### Acknowledgements

We thank Dr M. Bollen and G. Van der Hoeven (Laboratory Biosignaling & Therapeutics, Leuven, Belgium) for the generous gifts of the anti-PP1 monoclonal antibody and the plasmid coding for the PP1-binding domain of NIPP1; and V. Georget from Montpellier RIO Imaging for providing microscopy facilities. We also thank P. Richard and M. Plays from the Antibody Production Platform at the Centre de Recherche de Biochimie Macromoléculaire.

#### Competing interests

The authors declare no competing or financial interests.

#### Author contributions

This paper is submitted with the agreement of all its co-authors and the author list has been approved by all authors. S.M. performed all the experiments where FCP1 and PP1 were depleted. Experiments in which mitotic spindle and chromosome condensation were analysed, and *in vitro* dephosphorylation assays, as well as experiments for the revised version of the manuscript were performed by S.V. T.L. designed and performed experiments, discussed the results and wrote part of the manuscript. P.R. contributed to the experiments in which Thio-Arpp19 was used. A.C. wrote part of the manuscript and discussed the results. J.M.S. and S.C. performed and analysed mass spectrometry data.

#### Funding

This work was supported by the Ligue Nationale Contre le Cancer (Equipe Labellisée); the Agence Nationale de la Recherche [grant number ANR-10-BLAN-1207]; and the Fondation ARC pour la Recherche sur le Cancer [grant number PJA 20141201679]. S.M. is a Ministere de la Recherche fellow. P.R. is a Ligue Nationale Contre le Cancer fellow.

#### Supplementary information

Supplementary information available online at
http://jcs.biologists.org/lookup/suppl/doi:10.1242/jcs.178855/-/DC1

#### References

**Alvarez-Fernandez, M., Sanchez-Martinez, R., Sanz-Castillo, B., Gan, P. P., Sanz-Flores, M., Trakala, M., Ruiz-Torres, M., Lorca, T., Castro, A. and Malumbres, M.** (2013). Greatwall is essential to prevent mitotic collapse after nuclear envelope breakdown in mammals. *Proc. Natl. Acad. Sci. USA* **110**, 17374-17379.

**Blake-Hodek, K. A., Williams, B. C., Zhao, Y., Castilho, P. V., Chen, W., Mao, Y., Yamamoto, T. M. and Goldberg, M. L.** (2012). Determinants for activation of the atypical AGC kinase Greatwall during M phase entry. *Mol. Cell. Biol.* **32**, 1337-1353.

**Cundell, M. J., Bastos, R. N., Zhang, T., Holder, J., Gruneberg, U., Novak, B. and Barr, F. A.** (2013). The BEG (PP2A-B55/ENSA/Greatwall) pathway ensures cytokinesis follows chromosome separation. *Mol. Cell* **52**, 393-405.

**Gharbi-Ayachi, A., Labbe, J.-C., Burgess, A., Vigneron, S., Strub, J.-M., Brioudes, E., Van-Dorsselaer, A., Castro, A. and Lorca, T.** (2010). The substrate of Greatwall kinase, Arpp19, controls mitosis by inhibiting protein phosphatase 2A. *Science* **330**, 1673-1677.

**Grallert, A., Boke, E., Hagting, A., Hodgson, B., Connolly, Y., Griffiths, J. R., Smith, D. L., Pines, J. and Hagan, I. M.** (2015). A PP1-PP2A phosphatase relay controls mitotic progression. *Nature* **517**, 94-98.

**Hégarat, N., Vesely, C., Vinod, P. K., Ocasio, C., Peter, N., Gannon, J., Oliver, A. W., Novák, B. and Hochegger, H.** (2014). PP2A/B55 and Fcp1 regulate Greatwall and Ensa dephosphorylation during mitotic exit. *PLoS Genet.* **10**, e1004004.

**Lorca, T., Cruzalegui, F. H., Fesquet, D., Cavadore, J.-C., Mery, J., Means, A. and Dorée, M.** (1993). Calmodulin-dependent protein kinase II mediates inactivation of MPF and CSF upon fertilization of Xenopus eggs. *Nature* **366**, 270-273.

**Lorca, T., Bernis, C., Vigneron, S., Burgess, A., Brioudes, E., Labbe, J.-C. and Castro, A.** (2010). Constant regulation of both the MPF amplification loop and the Greatwall-PP2A pathway is required for metaphase II arrest and correct entry into the first embryonic cell cycle. *J. Cell Sci.* **123**, 2281-2291.

**Mochida, S., Ikeo, S., Gannon, J. and Hunt, T.** (2009). Regulated activity of PP2A-B55 delta is crucial for controlling entry into and exit from mitosis in Xenopus egg extracts. *EMBO J.* **28**, 2777-2785.

**Mochida, S., Maslen, S. L., Skehel, M. and Hunt, T.** (2010). Greatwall phosphorylates an inhibitor of protein phosphatase 2A that is essential for mitosis. *Science* **330**, 1670-1673.

**Peters, J.-M.** (2006). The anaphase promoting complex/cyclosome: a machine designed to destroy. *Nat. Rev. Mol. Cell Biol.* **7**, 644-656.

**Satinover, D. L., Leach, C. A., Stukenberg, P. T. and Brautigan, D. L.** (2004). Activation of Aurora-A kinase by protein phosphatase inhibitor-2, a bifunctional signaling protein. *Proc. Natl. Acad. Sci. USA* **101**, 8625-8630.

**Vigneron, S., Prieto, S., Bernis, C., Labbé, J.-C., Castro, A. and Lorca, T.** (2004). Kinetochore localization of spindle checkpoint proteins: who controls whom? *Mol. Biol. Cell* **15**, 4584-4596.

**Vigneron, S., Gharbi-Ayachi, A., Raymond, A.-A., Burgess, A., Labbe, J.-C., Labesse, G., Monsarrat, B., Lorca, T. and Castro, A.** (2011). Characterization of the mechanisms controlling Greatwall activity. *Mol. Cell. Biol.* **31**, 2262-2275.

**Williams, B. C., Filter, J. J., Blake-Hodek, K. A., Wadzinski, B. E., Fuda, N. J., Shalloway, D. and Goldberg, M. L.** (2014). Greatwall-phosphorylated Endosulfine is both an inhibitor and a substrate of PP2A-B55 heterotrimers. *Elife* **3**, e01695.

**Winkler, C., De Munter, S., Van Dessel, N., Lesage, B., Heroes, E., Boens, S., Beullens, M., Van Eynde, A. and Bollen, M.** (2015). The selective inhibition of protein phosphatase-1 results in mitotic catastrophe and impaired tumor growth. *J. Cell Sci.* **128**, 4526-4537.

**Wu, J. Q., Guo, J. Y., Tang, W., Yang, C.-S., Freel, C. D., Chen, C., Nairn, A. C. and Kornbluth, S.** (2009). PP1-mediated dephosphorylation of phosphoproteins at mitotic exit is controlled by inhibitor-1 and PP1 phosphorylation. *Nat. Cell Biol.* **11**, 644-651.